Ultrasound attenuation in s^{\pm} -wave two-band superconductors

ZHAO Runzhong, JIN Biao†

(School of Physical Sciences, University of Chinese Academy of Sciences Beijing 100049, China)

Abstract The two-band s^{\pm} -wave state is currently considered to be the most promising candidate for newly discovered iron-based high- T_c superconductors. In this work we study theoretically the ultrasound attenuation in s^{\pm} -wave two-band superconductors. The impurity effect is calculated within the \mathscr{T} -matrix approximation. In particular, our theory predict that, when the sizes of two order parameter are comparable, a Hebel-Slichter peak may show up in the ultrasound attenuation versus temperature curves. Our calculations also confirmed the presence of the resonant impurity scattering at low temperature, observed previously by other authors^[1] in the calculation of the NMR relaxation rate $1/T_1$.

Keywords Ultrasound attenuation; Iron-based superconductors; s^{\pm} -wave pairing; \mathscr{T} -matrix approximation

Introduction

The discovery of the high- T_c superconductivity in iron-based compounds has promoted highly intensive research activities in solid-state physics^[2–8]. The maximum T_c value of this iron-based family well exceeds that in MgB₂ and places them in the vicinity of cuprate superconductors. For this newly discovered family of high- T_c superconductors, the pairing symmetry of its superconducting gap is a key to understand the mechanism of superconductivity. Extensive experimental and theoretical work have been done to address this important issue for iron-based superconductors^[7,9,10].

From the experimental perspective, the situation is unclear. The NMR Knight shift indicates the spin-singlet state^[11–13]. The transition temperature T_c seems to be robust to impurity effects^[14]. While the penetration depth^[15], the specific heat^[16], and ARPES ^[17,18] indicate

almost isotropic two-gap system, the NMR relaxation rate $1/T_1$ shows no Hebel-Slichter coherent peak, nor the exponential decay at low temperature, but rather a power-like law, usually referred to as T^3 but in reality somewhere between T^3 and $T^{2.5}$, which suggest existence of line nodes [11, 12, 19, 20].

Among many theoretical research studies, the state mostly accepted as a standard pairing state of the iron-based superconductors is the spin singlet s-wave state with sign-changing order parameter (OP), arising from antiferromagnetic fluctuation^[21,22]. This state is currently referred to as the s^{\pm} -wave state. Sign-changing feature in the s^{\pm} -wave superconductor can produce some unique and distinct superconducting properties. In particular, many authors have attempted to provide a theoretical explanation for the puzzling $1/T_1$ data mentioned above based on the s^{\pm} -wave state^[1,23,24]. It is demonstrated that due to the sign-changing feature of the s^{\pm} -wave supercon-

 $^{^\}dagger$ Corresponding author, E-mail: biaojin@ucas.ac.cn

ductor, its Hebel-Slichter coherent peak is substantially suppressed intrinsically. The low temperature power-law-like behavior of $1/T_1$ is explained by the effect of formation of off-centered resonant bound state inside the superconducting gap by impurity scattering in the unitary limit^[25].

It is expected that the sign-changing feature of OP can also substantially affect the temperature dependence of the ultrasound attenuation α_s in s^{\pm} -wave superconductors since the coherence factors for $1/T_1$ and α_s are related closely similar to that in one-band case^[26]. However, no theoretical studies on ultrasound attenuation have been reported yet, to the best of our knowledge . It is the purpose of this work to narrow this gap.

1 Formalism

We start with the mean-field BCS Hamiltonian describing a two-band isotropic *s*-wave superconductor put forward by Suhl et al.^[27]:

$$H = \sum_{\mathbf{k},s} \varepsilon_{s\mathbf{k}} \left(c_{s,\mathbf{k}\uparrow}^{\dagger} c_{s,\mathbf{k}\uparrow} + c_{s,-\mathbf{k}\downarrow}^{\dagger} c_{s,-\mathbf{k}\downarrow} \right) - \sum_{\mathbf{k},s} \left(\Delta_{s} c_{s,\mathbf{k}\uparrow}^{\dagger} c_{s,-\mathbf{k}\downarrow}^{\dagger} + \Delta_{s} c_{s,-\mathbf{k}\downarrow} c_{s,\mathbf{k}\uparrow} \right)$$
(1)

where s(=1,2) denotes the band index, $\varepsilon_{s\mathbf{k}}$ is the energy of noninteracting state with respect to the chemical potential, and Δ_s , assumed to be a real quantity, is the OP defined by

$$\Delta_{s} = \sum_{\mathbf{k}',s'} V_{ss'} \langle c_{s',-\mathbf{k}'\downarrow} c_{s',\mathbf{k}'\uparrow} \rangle, \tag{2}$$

with $V_{ss'}$ being the effective electron-electron interaction within (s = s') or between $(s \neq s')$ the bands. The temperature dependence of Δ_s is determined by the coupled self-consistent gap equations

$$\Delta_s = \pi \sum_{s'} V_{ss'} N_{s'} T \sum_n \frac{\Delta_{s'}}{\sqrt{\omega_n^2 + \Delta_{s'}^2}}$$
(3)

for s=1 and 2. In the above, N_s is density of states of the sth band at Fermi energy, T denotes the temperature, and $\omega_n = \pi T (2n+1)$ is the Matsubara frequency.

Now we calculate the ultrasound attenuation coefficient α_s for our superconducting state using the standard formula^[26,28]:

$$\alpha_s \propto \lim_{\omega \to 0} \sum_{\mathbf{q}} \operatorname{Im} \Pi^R(\mathbf{q}, \omega)$$
 (4)

where $\Pi^R(\mathbf{q}, \boldsymbol{\omega})$ is Fourier transform of the retarded charge density correlation function

$$\Pi^{R}(\mathbf{q},t) = -i\theta(t)\langle [\hat{\boldsymbol{\rho}}(\mathbf{q},t), \hat{\boldsymbol{\rho}}(-\mathbf{q},0)]\rangle, \tag{5}$$

with

$$\hat{\rho}(\mathbf{q}) = \sum_{\mathbf{k},\sigma} c_{\mathbf{k}\sigma}^{\dagger} c_{\mathbf{k}+\mathbf{q}\sigma}.$$
 (6)

In practice, the correlation function is conveniently calculated in the Matsubara frequency domain,

$$\Pi(\mathbf{q}, i\mathbf{v}_m) = \sum_{\mathbf{k}, s, s'} T \sum_{n} \left(G_s(\mathbf{k}, i\boldsymbol{\omega}_n) G_{s'}(\mathbf{k} + \mathbf{q}, i\boldsymbol{\omega}_n + i\mathbf{v}_m) + G_s(-\mathbf{k}, -i\boldsymbol{\omega}_n) G_{s'}(-\mathbf{k} - \mathbf{q}, -i\boldsymbol{\omega}_n - i\mathbf{v}_m) \right)$$
(7)

where G_s and F_s denote the usual normal and anomalous single-particle Matsubara Green's functions. The summation over Matsubara frequency can be carried out with the help of the spectral representation of Green's functions, and the result is then analytically continued to the real frequency axis $iv_m \rightarrow \omega + i\delta$. We finally obtain

$$\frac{\alpha_{s}}{\alpha_{n}} = \int_{-\infty}^{\infty} d\omega \left(-\frac{\partial f}{\partial \omega} \right) \\
\left[\left(\sum_{s} \frac{N_{s}}{N_{tot}} \operatorname{Re} \frac{\omega}{\sqrt{\omega^{2} - \Delta_{s}^{2}}} \right)^{2} - \left(\sum_{s} \frac{N_{s}}{N_{tot}} \operatorname{Re} \frac{\Delta_{s}}{\sqrt{\omega^{2} - \Delta_{s}^{2}}} \right)^{2} \right]$$
(8)

where α_n stands for the attenuation coefficient corresponding to the normal state, $f(\omega)$ is the Fermi distribution function, and $N_{tot} = N_1 + N_2$.

2 Ultrasound attenuation in the clean limit

It is realized that, even for repulsive intraband and interband interactions ($V_{ij} < 0$) the above gap equations

produce the so-called s^{\pm} -wave solutions when the interband pairing interaction $V_{12}(=V_{21})$ is dominant over the intraband interaction $|V_{12}| > |V_{11}|, |V_{22}|^{[21,29]}$; in the s^{\pm} -wave state the two OPs acquire opposite signs. In this paper we will discuss the s^{\pm} -wave state focusing on the $|V_{12}| \gg |V_{11}| = |V_{22}|$ case.

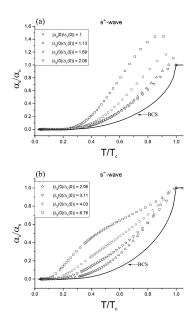


Fig. 1: Ultrasonic attenuation in clean $s\pm$ -wave superconductor with gap ratio (a) ≤ 2 , (b) ≥ 2 . One-band BCS result is shown with solid line for comparison.

Note that when $\Delta_1 = \Delta_2$, $N_1 = N_2$, Eq.(8) reproduces the BCS result of one-band s-wave superconductor, $\alpha_s/\alpha_n = 2f(\Delta(T))$, which decreases exponentially at low temperatures. In the two-band case, however, the situation can be qualitatively different due to the presence of the crossing term $\propto \Delta_1 \Delta_2$, especially when $\Delta_1 \Delta_2 < 0$. It is known that such a term (but with opposite sign) also shows up in the calculation of $1/T_1$ for the same s^{\pm} -model^[1] leading to strong reduction of the Hebel-Slichter peak. It is found that, in the case of the s^{\pm} -wave state α_s/α_n exhibits a marked Hebel-Slichter peak like $1/T_1$, in sharp contrast to the one-band case. We show in Fig. 1 the temperature dependence of α_s/α_n for various $|\Delta_2(0)/\Delta_1(0)|$, where $\Delta_s(0)$ is the zero-temperature value of the OP $\Delta_s(T)$. The solid line represents the BCS one-

band result. As can be seen, the Hebel-Slichter peak reduces rapidly as the ratio $|\Delta_2(0)/\Delta_1(0)|$ deviating from 1 (Fig. 1(a)). For $|\Delta_2(0)/\Delta_1(0)| > 2$, α_s/α_n exhibits typical behaviors of multiband superconductors; the fully gapped exponential dependence is visible only in the lowest temperature region (Fig. 1(b)).

3 Impurity effects

In this section, we investigate impurity effects on ultrasound attenuation employing the self-consistent \mathscr{T} -matrix approximation [30–32]. It is well-known that, as a low impurity density expansion rather than a coupling constant expansion, the \mathscr{T} -matrix approximation can be used to describe impurity scattering continuously from the Born (weak coupling) limit to the unitary (strong coupling) limit, hence can capture phenomena like the impurity resonance which does not possibly occur within the conventional Born approximation.

We consider an isotropic non-magnetic impurity scattering^[31] described by

$$H_{\text{imp}} = \sum_{i} \sum_{s,s',\mathbf{k},\mathbf{k}',\sigma} e^{i(\mathbf{k}-\mathbf{k}')\cdot\mathbf{R}_i} u_{ss'} c_{s\mathbf{k}\sigma}^{\dagger} c_{s'\mathbf{k}'\sigma}$$
(9)

where $u_{ss'}$ is single-impurity potential within (s=s') or between $(s \neq s')$ the bands, and \mathbf{R}_i is the position of the i-th impurity atom. Using the Green's function approach one can take into account the impurity effects systematically within the scope of \mathscr{T} -matrix approximation (see Appendix). In the following calculations, we consider the $u_{ij} = u$ case.

Now due to the impurity scattering, the gap equations (Eq.(3)) and the expression of the ultrasound attenuation coefficient (Eq.(8)) are modified to

$$\Delta_{s} = \pi \sum_{s'} V_{ss'} N_{s'} T \sum_{n} \frac{\tilde{\Delta}_{s'}}{\sqrt{\tilde{\omega}_{s'n}^{2} + \tilde{\Delta}_{s'}^{2}}}, \tag{10}$$

and

$$\frac{\alpha_{s}}{\alpha_{n}} = \int_{-\infty}^{\infty} d\omega \left(-\frac{\partial f}{\partial \omega} \right) \\
\left[\left(\sum_{s} \frac{N_{s}}{N_{tot}} \operatorname{Re} \frac{\tilde{\omega}_{s}}{\sqrt{\tilde{\omega}_{s}^{2} - \tilde{\Delta}_{s}^{2}}} \right)^{2} \\
- \left(\sum_{s} \frac{N_{s}}{N_{tot}} \operatorname{Re} \frac{\tilde{\Delta}_{s}}{\sqrt{\tilde{\omega}_{s}^{2} - \tilde{\Delta}_{s}^{2}}} \right)^{2} \right].$$
(11)

In the above, $\tilde{\omega}_s$ and $\tilde{\Delta}_s$ denote respectively the renormalized frequency and energy gap

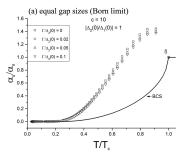
$$\tilde{\omega}_{\rm s} = \omega + i\Sigma_{\rm s}^0(\omega),\tag{12}$$

$$\tilde{\Delta}_s = \Delta_s + \Sigma_s^1(\omega), \tag{13}$$

with $\Sigma_s^0(\omega)$ and $\Sigma_s^1(\omega)$ being the impurity self-energy corrections to be determined in a self-consistent manner (see Appendix).

In discussing the impurity effects it is convenient to introduce two dimensionless parameters defined by $\Gamma = n_{\rm imp}/(\pi N_{tot})$ and $c = 1/(\pi N_{tot}u)$ where $n_{\rm imp}$ denotes the impurity concentration. Evidently, Γ measures the impurity concentration and c the scattering strength. The Born limit and the unitary limit correspond to $c \gg 1$ and $c \to 0$, respectively.

We study first the effect of impurity scattering in the Born limit (c=10). Plotted in Fig. 2(a) and Fig. 2(b) are the temperature variation of α_s/α_n under different impurity concentration Γ for $|\Delta_2(0)/\Delta_1(0)|=1$, and $|\Delta_2(0)/\Delta_1(0)|=1.8$, respectively. The one-band BCS result (the solid line) is also shown for the sake of comparison; within the \mathscr{T} -matrix approximation, the Anderson's theorem $[^{33}]$ is valid for one-band s-wave state leading to α_s/α_n unaffected by non-magnetic impurity scattering (see Appendix). Clearly, α_s/α_n is rather robust for non-magnetic impurity scattering for s^\pm -wave superconductors in the Born limit .



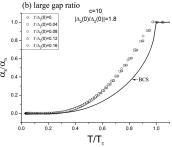


Fig. 2: Ultrasound attenuation in the Born limit with (a) equal gap sizes and (b) moderate gap ratio. Equal strength of intra- and inter-band scattering potential assumed. One-band BCS result is shown with solid line for comparison.

Next let us turn to the case of unitary limit (c=0). Displayed in Fig. 3 (a) and Fig. 3(b) are the temperature variation of α_s/α_n under different impurity concentration Γ for $|\Delta_2(0)/\Delta_1(0)| = 1$, and $|\Delta_2(0)/\Delta_1(0)| = 1.8$, respectively. In the $|\Delta_2(0)/\Delta_1(0)| = 1$ case, the α_s/α_n as a whole, and the Hebel-Slichter coherence peak in particular, are suppressed with the increment of impurity concentration Γ (Fig. 3(a)). In the $|\Delta_2(0)/\Delta_1(0)| = 1.8$ case, however, the temperature dependence of α_s/α_n is characterized by the absence of the Hebel-Slichter coherence peak, and the strong deviation from the fully gapped one-band behaviour at low temperatures due to the resonant impurity scattering ^[25]. Finally, we also have studied the cases with $|\Delta_2(0)/\Delta_1(0)| > 4$, and found that α_s/α_n is almost unaffected by impurity scattering both in the Born and unitary limits.

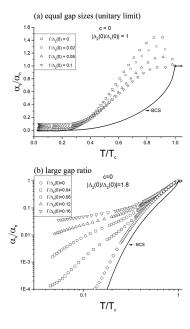


Fig. 3: Ultrasound attenuation in the unitary limit with (a) equal gap sizes and (b) moderate gap ratio. Equal strength of intra- and inter-band scattering potential assumed. One-band BCS result is shown with solid line for comparison.

4 Conclusion

In this work, we have investigated the temperature dependence of the ultrasound attenuation coefficient, α_s/α_n , in the s^{\pm} -wave two-band superconductors with or without impurity scattering. In discussing the impurity effects we have used the existing self-consistent T-matrix approximation, and considered both the Born and unitary limits. The important observation of this work is that, when the sizes of two order parameter are comparable, a Hebel-Slichter peak may emerge in the α_s/α_n-T curves, in strong contrast to one-band case. This coherence peak is robust for impurity scattering in the Born limit, but suppressed moderately with the impurity concentration in the unitary limit. Experimental investigation on this issue is highly desired. Besides, when $|\Delta_2(0)/\Delta_1(0)|$ is large, α_s/α_n exhibit non-exponential-decay behaviors at low temperature, in consistent with that observed for $1/T_1$ in the previous theoretical investigations.

Appendix: \mathcal{T} -matrix approximation

For a two-band *s*-wave superconductor subjected to impurity scattering described by Eq.(9), the impurity-averaged total single-particle Matsubara Green's function can be written as

$$\hat{G}_s^{-1}(\mathbf{k}, i\omega_n) = \hat{G}_s^{-1}(\mathbf{k}, i\omega_n) - \hat{\Sigma}_s(i\omega_n), \tag{14}$$

where \hat{G}_s is the Nambu Green's function in the absence of impurity scattering

$$\hat{G}_{s}(\mathbf{k}, i\omega_{n}) = -\frac{i\omega_{sn}\hat{\tau}^{0} + \varepsilon_{s\mathbf{k}}\hat{\tau}^{3} + \Delta_{s}\hat{\tau}^{1}}{\omega_{sn}^{2} + \varepsilon_{s\mathbf{k}}^{2} + \Delta_{s}^{2}}$$
(15)

with $\hat{\tau}^i(i=0,1,2,3)$ the Pauli matrices, and $\hat{\Sigma}_s(i\omega_n)$ the total self-energy matrix to be solved. We can expand the self-energy in the form^[32]:

$$\hat{\Sigma}_s = \sum_i \Sigma_s^i \hat{\tau}^i \tag{16}$$

with $\Sigma_s^2 = \Sigma_s^3 = 0$. In our \mathscr{T} -matrix approximation, where processes involving scattering from multiple impurity sites are ignored, the self energy is obtained by multiplying the single-impurity contribution by the impurity concentration, reflecting the multiple-scattering effect. [34]

$$\Sigma_s^i(i\omega_n) = n_{\text{imp}} \cdot \mathscr{T}_s^i(\omega_n)$$
 (17)

where \mathcal{T}_s^i is the $\hat{\tau}^i$ component of the \mathcal{T} -matrix $\hat{\mathcal{T}}_s$. In the two-band s-wave case, the equations for the \mathcal{T} -matrix for band 1 are given by (see Fig.(4) for a diagrammatic description)

$$\hat{\mathcal{T}}_{1}(i\omega_{n}) = \hat{u}_{11} + \sum_{\mathbf{k}} \hat{u}_{11} \hat{G}_{1}(\mathbf{k}, i\omega_{n}) \hat{\mathcal{T}}_{1}(i\omega_{n})
+ \sum_{\mathbf{k}} \hat{u}_{12} \hat{G}_{2}(\mathbf{k}, i\omega_{n}) \hat{\mathcal{T}}_{21}(i\omega_{n})
\hat{\mathcal{T}}_{21}(i\omega_{n}) = \hat{u}_{21} + \sum_{\mathbf{k}} \hat{u}_{21} \hat{G}_{1}(\mathbf{k}, i\omega_{n}) \hat{\mathcal{T}}_{1}(i\omega_{n})
+ \sum_{\mathbf{k}} \hat{u}_{22} \hat{G}_{2}(\mathbf{k}, i\omega_{n}) \hat{\mathcal{T}}_{21}(i\omega_{n}).$$
(18)

Combining these equations above, one can obtain

$$\begin{split} \mathscr{T}_{1}^{0} &= -\frac{i}{D} \left[u_{11}^{2} g_{1,0} + u_{12}^{2} g_{2,0} \right. \\ &+ g_{1,0} (u_{12}^{2} - u_{11} u_{22})^{2} (g_{2,0}^{2} + g_{2,1}^{2}) \right] \\ \mathscr{T}_{1}^{1} &= \frac{1}{D} \left[u_{11}^{2} g_{1,1} + u_{12}^{2} g_{2,1} \right. \\ &+ g_{1,1} (u_{12}^{2} - u_{11} u_{22})^{2} (g_{2,0}^{2} + g_{2,1}^{2}) \right] \end{split}$$

where

$$D = 1 + u_{11}^2 (g_{1,0}^2 + g_{1,1}^2) + u_{22}^2 (g_{2,0}^2 + g_{2,1}^2)$$

+ $2u_{12}^2 (g_{1,0}g_{2,0} + g_{1,1}g_{2,1})$
+ $(u_{12}^2 - u_{11}u_{22})^2 (g_{1,0}^2 + g_{1,1}^2) (g_{2,0}^2 + g_{2,1}^2)$

$$g_{s,0} = \sum_{k} \frac{i}{2} \operatorname{tr} \hat{\tau}^{0} \hat{\tilde{G}}_{s}(k, i\omega_{n}) = \pi N_{s} \frac{\tilde{\omega}_{sn}}{\sqrt{\tilde{\omega}_{sn}^{2} + \tilde{\Delta}_{s}^{2}}}$$

$$g_{s,1} = \sum_{k} \frac{1}{2} \operatorname{tr} \hat{\tau}^{1} \hat{\tilde{G}}_{s}(k, i\omega_{n}) = \pi N_{s} \frac{\tilde{\Delta}_{s}}{\sqrt{\tilde{\omega}_{sn}^{2} + \tilde{\Delta}_{s}^{2}}}$$
(20)

with the Matsubara frequency and gap functions renormalized as

$$\tilde{\omega}_{sn} = \omega_n + i\Sigma_s^0(\omega_n)$$

$$\tilde{\Delta}_s = \Delta_s + \Sigma_s^1(\omega_n)$$
(21)

The \mathscr{T} -matrices for the second band can be obtained by interchanging the band indices $1 \leftrightarrow 2$.

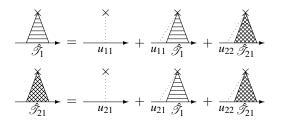


Fig. 4: Self-energy correction to Green's function in band 1 within the \mathscr{T} -matrix approximation. The cross (\times) denotes the impurity site, and the solid line is impurity averiged Green's function.

In practice, one can solve Eqs. (17) and (19) together with the coupled gap equations

$$\Delta_{s} = \pi \sum_{s'} V_{ss'} N_{s'} T \sum_{n} \frac{\Delta_{s'}}{\sqrt{\tilde{\omega}_{s'n}^{2} + \tilde{\Delta}_{s'}^{2}}}$$
(22)

self-consistently for \mathcal{T}_1^0 , \mathcal{T}_1^1 , Δ_1 , and Δ_2 , at different Matsubara frequencies, and then obtain the retarded self-energies either via analytic continuation or by making use of the so-called Padé approximants^[1,35].

References

(19)

- [1] Bang Y. Choi H.Y. Won H., Phys Rev B, 79(2009), 054529
- [2] Stewart G.R., Rev. Mod. Phys, 83(2011), 1589
- [3] Wang N.L. Hosono H. Dai P.C., Iron-based Superconductors (Pan Stanford Publishing Pte Ltd, Singapore, 2013)
- [4] Hirschfeld P.J. Korshunov M.M. Mazin I.I., Rep Prog Phys, 74(2011), 124508
- [5] Chubukov A. Hirschfeld P.J., Physics Today, 68(6)(2015), 46
- [6] Hosono H. Kuroki K., Physica C, 514(2015), 399
- [7] Hirschfeld P.J. Comptes Rendus Physique, 17(2016), 197
- [8] Bang Y. Stewart G.R., J Phys Condens Matter, 29(2017), 123003
- [9] Johnston D.C., Advances in physics, 59(2010), 8031061
- [10] Richard P. Qian T. Ding H., J Phys: Condens Matter, 27(2015), 293203
- [11] Matano K. Ren Z.A. Dong X.L. et al., Europhys Lett, 83(2008), 57001
- [12] Grafe H.J. Paar D. Lang G. et al., Phys Rev Lett, 101(2008), 047003
- [13] Ning F. Ahilan K. Imai T. et al., J Phys Soc Jpn, 77(2008), 103705
- [14] Kawabata A. Lee S.C. Kobayashi Y. et al., J Phys Soc Jpn, 77(2008), 103704

- [15] Hashimoto K. Shibauchi T. Kato T. et al., Phys Rev [25] Bang Y., EPJ Web of Conferences, 23(2012), 00010 Lett, 102(2009), 017002
- [16] Mu G. Luo H.Q. Wang Z.S. et al., Phys Rev B, 79(2009), 174501
- [17] Ding H. Richard P. Nakayama K. et al., Europhys Lett, 83(2008), 47001
- [18] Kondo K. Santander-Syro A. F. Copie O. et al., Phys Rev Lett, 101(2008), 147003
- [19] Nakai Y. Ishida K. Kamihara Y. et al., J Phys Soc Jpn, 77(2008), 073701
- [20] Mukuda H. Terasaki N. Kinouchi H. et al., J Phys Soc Jpn, 77(2008), 093704
- [21] Mazin I.I., Singh D.J. Johannes M.D. et al., Phys Rev Lett, 101(2008), 057003
- [22] Kuroki K. Onari S. Arita R. et al., Phys Rev Lett, 101(2008), 087004
- [23] Parker D. Dolgov O.V. Korshunov M.M. et al., Phys Rev B 78(2008), 134524
- [24] Chubukov A.V. Efremov D.V. Eremin I., Phys Rev B, 78(2008), 134512

- [26] Schrieffer J.R., Theory of Superconductivity (Benjamin, New York, 1964)
- [27] Suhl H. Mattias B.T. Walker L.R., Phys Rev Lett, 3(1959): 552
- [28] Nayak N., Quantum Condensed Matter Physics Lecture Notes (http://stationq.cnsi.ucsb. edu/ nayak/qft-9-29-2011.pdf, 2011)
- [29] Golubov A.A. Mazin I.I., Physica C, 243(1995), 153
- [30] Hirschfeld P.J. Wolfle P. Einzel D., Phys Rev B, 37(1988), 83
- [31] Ohashi Y., Physica C, 412-414(2004), 41
- [32] Mishra V. Vorontsov A. Hirschfeld P.J. et al., Phys Rev B, 80(2009), 224525
- [33] Anderson P.W., J Phys Cem Solid, 11(1959), 26
- [34] Mahan G.D., Many-particle Physics (Springer Science+Bussiness Media, New York, 2000)
- [35] Vidberg H.J. Serene J.W., J Low Temp Physics, 29(1977), 179192